

CHAPTER-II

**REFRACTIVE INDEX MEASUREMENTS AND X-RAY DIFFRACTION STUDIES ON
MESOGENIC SUBSTANCES : THEORETICAL BACKGROUNDS AND EXPERIMENTAL
TECHNIQUES**

2.1

REFRACTIVE INDEX MEASUREMENTS

2.1.1 Theory

An uniaxial liquid crystal has two principal refractive indices, n_o and n_e . In the case of a nematic or a uniaxial smectic liquid crystal the optical axis is given by the director. The terms n_{\parallel} and n_{\perp} are used for the directions parallel and perpendicular to the director. We therefore have

$$n_o = n_{\perp} \quad \text{and} \quad n_e = n_{\parallel}$$

From the measurement of n_o and n_e we can estimate ordering in the liquid crystal at different temperatures.

In a liquid crystal the polarization \bar{P} is given by

$$\bar{P} = N \langle \bar{\alpha} \cdot E_i \rangle,$$

where the brackets denote the average over the orientations of all molecules. $\bar{\alpha}$ is the molecular polarizability, N is the number of molecules per unit volume and E_i is the internal field, the average field that acts on a molecule.

The internal field is a linear function of the macroscopic field and its relation to macroscopic field can be represented by

$$E_i = \bar{K} \cdot E,$$

where \bar{K} is an ordinary second-rank tensor. The introduction of this tensor makes it possible to write $\bar{P} = N \langle \bar{\alpha} \cdot \bar{K} \rangle \cdot E$.

Refractive index is related to polarizability by the following

relation

$$n_{\parallel}^2 - n_{\perp}^2 = N \left[\langle \bar{\alpha} \cdot \bar{K} \rangle_{\parallel} - \langle \bar{\alpha} \cdot \bar{K} \rangle_{\perp} \right]$$

So if we want to calculate molecular polarizability we must know the internal field tensor \bar{K} . Lorentz-Lorentz derived equations relating polarizability and refractive indices based on models for \bar{K} which was usually valid for isotropic medium. Because of the anisotropy of the internal field, Lorentz-Lorentz formula can't be applied to liquid crystals. We follow, therefore, Neugebauer's relations¹ or Vuks' formula² to calculate the polarizabilities.

Neugebauer's Relations

Neugebauer's relations to calculate the effective polarizabilities α_o and α_e of the liquid crystals are given by

$$n_o^2 - 1 = 4\pi N \alpha_o (1 - N \alpha_o \gamma_o)^{-1} \quad (1)$$

$$n_e^2 - 1 = 4\pi N \alpha_e (1 - N \alpha_e \gamma_e)^{-1} \quad (2)$$

where N is the number of molecules per c.c. and γ_o and γ_e are internal field constants for ordinary and extraordinary rays respectively with their respective polarizabilities α_o and α_e .

The relevant equations for calculating the polarizabilities α_o and α_e obtained from equations (1) and (2) are

$$1/\alpha_o + 2/\alpha_e = \frac{4\pi N}{3} \left[\frac{(n_e^2 + 2)}{(n_e^2 - 1)} + \frac{2(n_o^2 + 2)}{(n_o^2 - 1)} \right] \quad (3)$$

$$\text{and } \alpha_e + 2\alpha_o = \frac{9}{4\pi N} \left[\frac{n^2 - 1}{n^2 + 2} \right] \quad (4)$$

Vuks' Formula

The Vuks' formula relating the principal polarizabilities and the refractive indices can be written as

$$\frac{n_i^2 - 1}{n^2 + 4} = \frac{4\pi}{3} N\alpha_i, \quad i = X, Y, Z. \quad (5)$$

$$\text{where } n^2 = 1/3 \sum_i n_i^2 \quad (6)$$

So we find

$$\frac{n_o^2 - 1}{n^2 + 2} = \frac{4\pi}{3} N\alpha_o \quad (7)$$

$$\frac{n_e^2 - 1}{n^2 + 2} = \frac{4\pi}{3} N\alpha_e \quad (8)$$

where $n^2 = (2n_o^2 + n_e^2)/3$; n being mean refractive index.

The relation between the order parameter $\langle P_2 \rangle$ and polarizabilities (α_o, α_e) is given by³

$$\alpha_e = \alpha + 2/3 \alpha_a \langle P_2 \rangle \quad (9)$$

$$\alpha_o = \alpha - 1/3 \alpha_a \langle P_2 \rangle \quad (10)$$

where $\alpha = (2\alpha_o + \alpha_e)/3$ is the mean polarizability and $\alpha_a = (\alpha_{||} - \alpha_{\perp})$

is the molecular polarizability anisotropy.

$$\text{So, } \langle P_2 \rangle = \frac{\alpha_e - \alpha_o}{\alpha_{\parallel} - \alpha_{\perp}} \quad (11)$$

To get the value of $(\alpha_{\parallel} - \alpha_{\perp})$ we followed Haller's extrapolation procedure⁴.

Haller's Extrapolation Procedure

$\ln(\alpha_e - \alpha_o)$ is plotted against $\ln(T_c - T)$ and a straight line is obtained. The value of $(\alpha_{\parallel} - \alpha_{\perp})$ is determined by extrapolating it to $\ln T_c$ (i.e. $T = 0$) so that $\langle P_2 \rangle = 1$ at that point where $(\alpha_e - \alpha_o)_{T=0} = (\alpha_{\parallel} - \alpha_{\perp})$.

Additive Rule of Bond Polarizability

Denbigh-Le Fevre established a simple sum rules for the calculation of molecular polarizability in terms of mean bond polarizability. Molecular polarizabilities for all the substances have been calculated from this additive rule and compared them with the values obtained from Vuks' and Neugebauer's methods.

2.1.2 EXPERIMENTAL PROCEDURE

Refractive indices were measured using thin prism of refracting angle of about 1° . The technique of the preparation of the thin prism is given in detail by Zeminder et al⁵. At first, the clean optically flat glass plates were rubbed parallel to one of their edges. The plates were then treated with aqueous solution of 1% polyvinyl alcohol and dried. Again they were rubbed along the same direction as before. The process of rubbing was repeated

several times. The prism was formed keeping the treated surfaces inside and the rubbing directions parallel to the refracting edge. The prism was precalibrated by measuring the refractive indices of distilled water, glycerine and potassium chromate solutions. The results were in good agreement with that obtained from Abbe's refractometer. Now the liquid crystal sample was allowed to flow inside the prism by melting a few crystals at the top. The sample inside the prism was heated to isotropic state and then cooled down very slowly in the presence of a magnetic field of strength 0.6 Tesla, keeping the edge of the prism parallel to the field. This process was repeated several times. We thus obtained a homogeneous specimen with the optic axis parallel to the refracting edge of the prism. The prism was kept inside a brass thermostat heated electrically and controlled by a temperature controller (Indotherm model 401) within $\pm 0.5^{\circ}\text{C}$. A precision spectrometer and a nicol prism were used to measure the refractive indices (n_o , n_e) within ± 0.001 for four different wavelengths from a mercury lamp.

The densities of the liquid crystalline phases at different temperatures were determined by putting weighed samples inside a dilatometer. It was placed in water bath for the samples having isotropic state within 100°C and for the samples having isotropic state above 200°C , a temperature controlled olive oil bath was used. The heights of the columns were measured at different temperatures during heating and cooling with the help of the travelling microscope. An interval of 30 minutes was allowed to attain the desired temperatures.

2.2 X-RAY DIFFRACTION STUDY

2.2.1 Theory and General Backgrounds

X-ray diffraction provides a powerful tool for the structural characterization of most materials. From this study we can verify the phase behaviour where it is extremely valuable. We may also determine layer and molecular spacings and correlation lengths. We can have thus a valuable insight into the molecular packing and a measure of the extent of order. Molecular parameters require in essence, only measurement of positions and widths of diffraction maxima. Qualitative aspects of distribution functions can also be determined from these diffraction patterns.

The diffraction experiments were first performed by Lingen⁶ and Friedel⁷. Vainshtein⁸ and Leadbetter⁹ have given theoretical interpretations.

Average Intermolecular Distance, Apparent Molecular Length and Layer Spacing

X-ray studies base their interpretations on normal-beam photographs of aligned or unaligned mesomorphic phases. Data on unoriented specimens can be very useful for initial characterization of samples and for obtaining intermolecular spacings, molecular lengths etc. I have determined molecular parameters using both aligned samples and powder specimen. Results of this study will be discussed in next chapter III.

The main features of small angle X-ray pattern of the sample oriented perpendicular to the incident X-ray is that the main halo splits into two crescents for each of which intensity is maximum in the equatorial direction. These crescents are mainly due to the

intermolecular scattering, the Bragg spacing being the lateral distance between the molecules. In the meridional section small angle rings observed are related to the apparent molecular length.

In general, the spacing X between two successive reflecting points or planes is related to the corresponding diffraction angle (2θ) by a formula given by¹⁰

$$2X \cdot \sin\theta = K \cdot \lambda \quad (12)$$

where λ = wavelength of the X-ray; K = constant depending on shape and arrangement of molecules¹¹. A. de Vries^{12,13} has discussed this equation (12), its applications and limitations in detail. In our cases we used $k = 1$ in equation (12) for the long spacings (i.e. apparent molecular length l in case of nematic and layer spacing d in case of smectic). For both the oriented and unoriented samples the value of k in equation (12) is taken to be 1.117 to calculate the intermolecular distance D .

Orientational Distribution Functions and Order Parameters

For a system of cylindrically symmetric molecules one can define an orientational distribution function $f(\beta)$, which gives an average state of orientation of the long axis of the molecules relative to the director¹⁴. From the X-ray diffraction photographs we get intensities averaged over a relatively long time and over a macroscopic volume so that it can be assumed that the molecules have an averaged cylindrical symmetry even if they do not rotate about their long axes¹⁵. The order parameters $\langle P_L \rangle$ for a system of rigid rods in a uniaxial phase are defined as

$$\langle P_L \rangle = \frac{\int_0^{\pi/2} P_L(\cos\beta) f(\beta) \sin\beta \, d\beta}{\int_0^{\pi/2} f(\beta) \sin\beta \, d\beta} \quad (13)$$

where $P_L(\cos\beta)$ is well known Legendre polynomial of order L . Putting $L = 2$ and $L = 4$ we get $\langle P_2 \rangle$ and $\langle P_4 \rangle$ from equation (13). In relating the X-ray intensities $I(\psi)$ around the diffuse equatorial arc (Figure 2.1) with the orientational distribution function, Leadbetter and Norries¹⁵ assumed the molecules as rigid rods perfectly aligned in clusters of a small number of molecules and obtained

$$I(\psi) = C \int_{\beta=\psi}^{\pi/2} f_d(\beta) \sec^2\psi \left[\tan^2\beta - \tan^2\psi \right]^{-1/2} \sin\beta \, d\beta \quad (14)$$

where $f_d(\beta)$ describes the distribution function of the clusters in which the molecules are perfectly aligned. Moreover, they assumed that for a perfectly aligned sample $[f_d(\beta) = \delta(\beta)]$, the scattering is zero except for the directions of the scattering vector perpendicular to the cluster axis. They have calculated the effects showing the deviations are negligible except for highly ordered phases ($\langle P_2 \rangle \geq 0.8$). Comparing the values of $f_d(\beta)$ with $f(\beta)$ of the same sample obtained by other methods it has been seen that $f_d(\beta)$ can be replaced by $f(\beta)$ values, the true singlet distribution function.

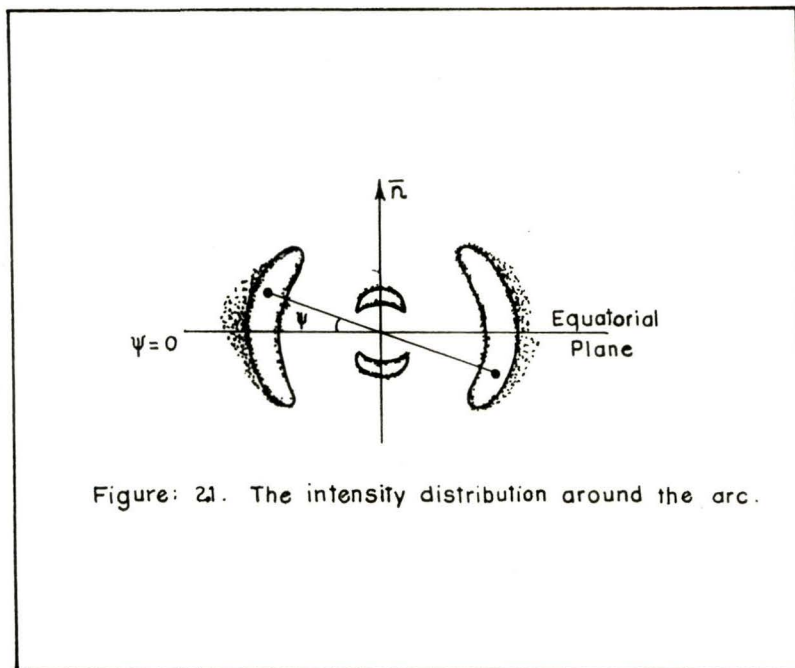


Figure: 21. The intensity distribution around the arc.

Because of centro-symmetric molecular distribution in nematic phase, the orientational distribution function can be expanded in the form^{15,16}

$$I(\psi) = \sum_{n=0}^r a_{2n} \cos^{2n} \psi \quad (15)$$

$$f(\beta) = \sum_{n=0}^r b_{2n} \cos^{2n} \beta \quad (16)$$

substituting $\sin \alpha = \cos \beta \sec \psi$ in equation (14) we get

$$I(\psi) = C \int_0^{\pi/2} f_1(\alpha) \sin \alpha \, d\alpha \quad (17)$$

From equations (15), (16) and (17) we have

$$\begin{aligned} \sum_{n=0}^r a_{2n} \cos^{2n} \psi &= \int_0^{\pi/2} \sum_{n=0}^r b_{2n} \cos^{2n} \psi \sin^{2n+1} \alpha \, d\alpha \\ &= \sum_{n=0}^r b_{2n} \cos^{2n} \psi \int_0^{\pi/2} \sin^{2n+1} \alpha \, d\alpha \end{aligned} \quad (18)$$

Since ψ is arbitrary, the coefficient of $\cos^{2n} \psi$ must be equal.

$$\text{Now} \quad \int_0^{\pi/2} \sin^{2n+1} \alpha \, d\alpha = \frac{2^{2n} (n!)^2}{(2n+1)!}$$

and so
$$b_{2n} = a_{2n} \cdot \frac{(2n+1)!}{2^{2n} (n!)^2} \quad (19)$$

The series in equations (15) and (16) converge rapidly. Retaining eight terms in the truncated series, a least square fitting was made to obtain the coefficients from equation (15) with corrected intensity values. The calculated intensity values in all cases were found to be in good agreement with the observed intensities. These values of a_{2n} were then used to calculate the coefficients of b_{2n} . Then, $f(\beta)$ values were calculated using eight terms in the series in equation (16).

By calculating the integral

$$\int_0^{\pi/2} f(\beta) \sin\beta \, d\beta = A \quad (\text{say}),$$

and then dividing all the b_{2n} values by A we obtained the normalized values of the orientational distribution function.

Substituting equation (16) in equation (13) we get

$$\langle P_2 \rangle = \frac{1}{2} \frac{\int_0^1 (3 \cos^2 \beta - 1) \sum_{n=0}^r b_{2n} \cos^{2n} \beta \, d(\cos \beta)}{\int_0^1 \sum_{n=0}^r b_{2n} \cos^{2n} \beta \, d(\cos \beta)} \quad (21)$$

This can be written in the form of standard integrals and $\langle P_2 \rangle$ can

be calculated. Similarly, $\langle P_4 \rangle$ can also be calculated. Vainshtein⁸ obtained a fairly good approximation for the order parameter by replacing $f(\beta)$ values with $I(\psi)$ values at a certain Bragg angle in equation (13).

2.2.2 EXPERIMENTAL TECHNIQUE AND DATA ANALYSIS

In this study flat plate method has been used. The flat plate camera equipped with high temperature arrangement was designed and fabricated by Jha et al¹⁷ in our laboratory. The set up has the provisions for interchangeable collimator, changable spacer to vary the sample to film distance and changable gap between pole pieces of the electromagnet. All the materials used are non-magnetic. Figure 2.2 shows the sectional diagram of the whole arrangement.

The temperature of the sample was regulated within $\pm 0.5^{\circ}\text{C}$ by a temperature controller (Indotherm model401). A sensitive Gaussmeter (ECIL model GHB67) was used to measure the strength of the magnetic field between the pole pieces. Ni filter of thickness 0.009 mm. was used for all the photographs to obtain nearly monochromatic CuK_{α} radiation of wavelength 1.5418 \AA . The X-ray beam was collimated by a collimator of aperture of 0.5 mm. The exact distance between the film and the sample was determined by taking aluminium powder pattern.

Conversion of Optical Density to X-Ray Intensity

The X-ray diffraction photographs were scanned both linearly and circularly with a Carl Zeiss Microdensitometer (MD 100) which has potentiometric recording (K 200) facility for linear scanning. The circular scanning was done manually with a rotation stage modified to enable 360° scan. The optical density values obtained

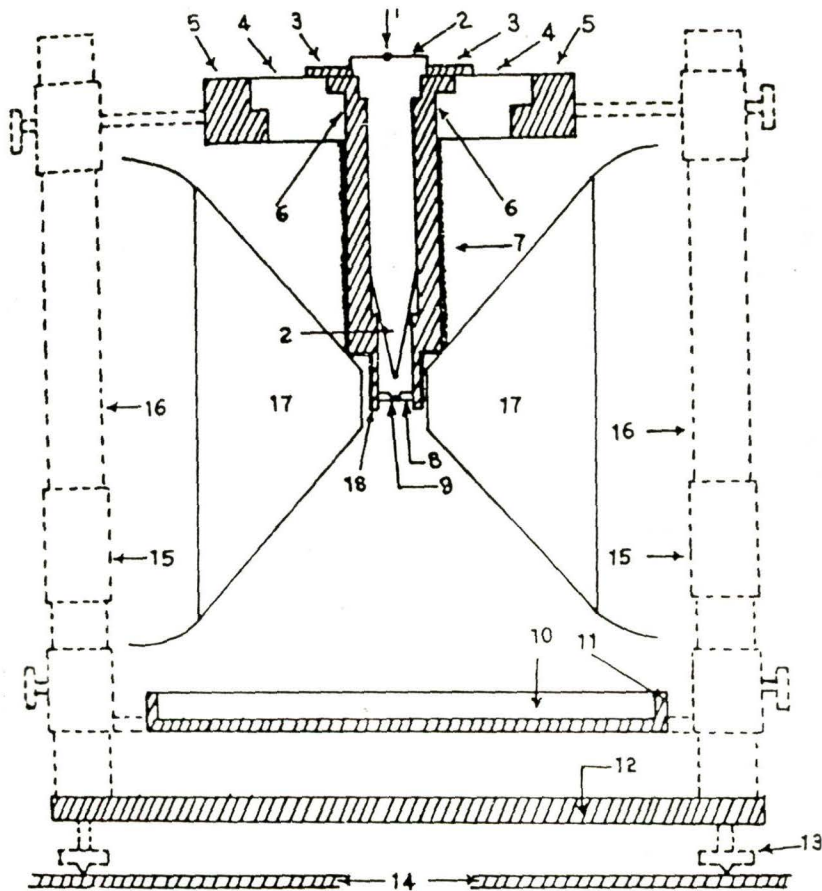


Fig 2.2 Sectional diagram of the camera:

(1) X-Ray; (2) Collimator; (3) Brass Ring; (4) Ring of Syndanio Board; (5) Brass Ring; (6) Cylindrical Brass Chamber; (7) Asbestos Insulation and Heater Winding; (8) Specimen Holder and Thermocouple; (9) Specimen; (10) Film Cassette; (11) Film Cassette Holder; (12) Base Plate; (13) Levelling Screw; (14) Brass Plates over the Coils of Electromagnet; (15) Removable Spacer; (16) Supporting Brass Stands; (17) Polepieces; (18) Asbestos insulation.

from the densitometric scan were converted to relative intensity values by a method explained by Klug and Alexander¹⁸. An intensity scale was prepared by exposing different portion of a film to X-rays coming through a small rectangular aperture. Multiple film technique was used. Optical density values of these spots were then measured with the microdensitometer and after subtracting the optical density of the unexposed film a calibration graph was prepared which is shown in the Figure 2.3.

Linear Scanning

Diameters of the diffraction rings were determined from the peak positions obtained by linear scanning using a chart drive. One such scanning is shown in Figure 2.4. After knowing the diameter, the bragg angle corresponding to this diffraction is determined from the equation

$$\tan 2\theta' = \frac{\text{Radius of the ring}}{\text{Sample to film distance}} \quad (22)$$

The molecular parameters were determined from equation (12).

Circular Scanning

To determine the orientational distribution function $f(\beta)$ and order parameters $\langle P_2 \rangle$ and $\langle P_4 \rangle$ circular scan of the outer diffraction ring is to be done. The values of the optical density obtained from the microdensitometric circular scan were converted to X-ray intensities with the help of the calibration curve. The converted intensity values were plotted against azimuthal angular positions. The intensity values were corrected for the background

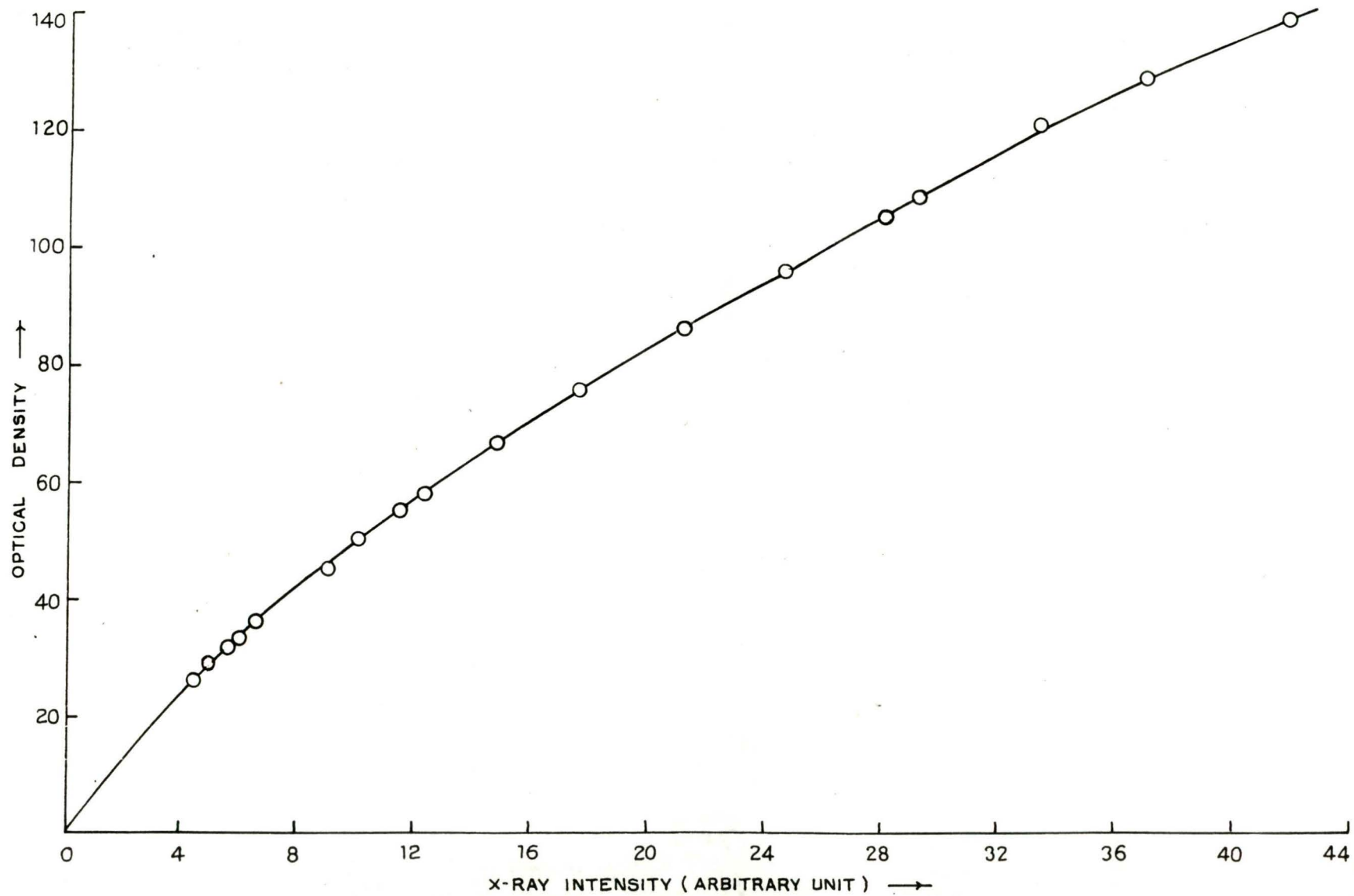


Figure 2.3 Optical density vs. X-ray intensity curve.

Sample HCCPP/84°C
Magnetic Field: 0.6 Tesla

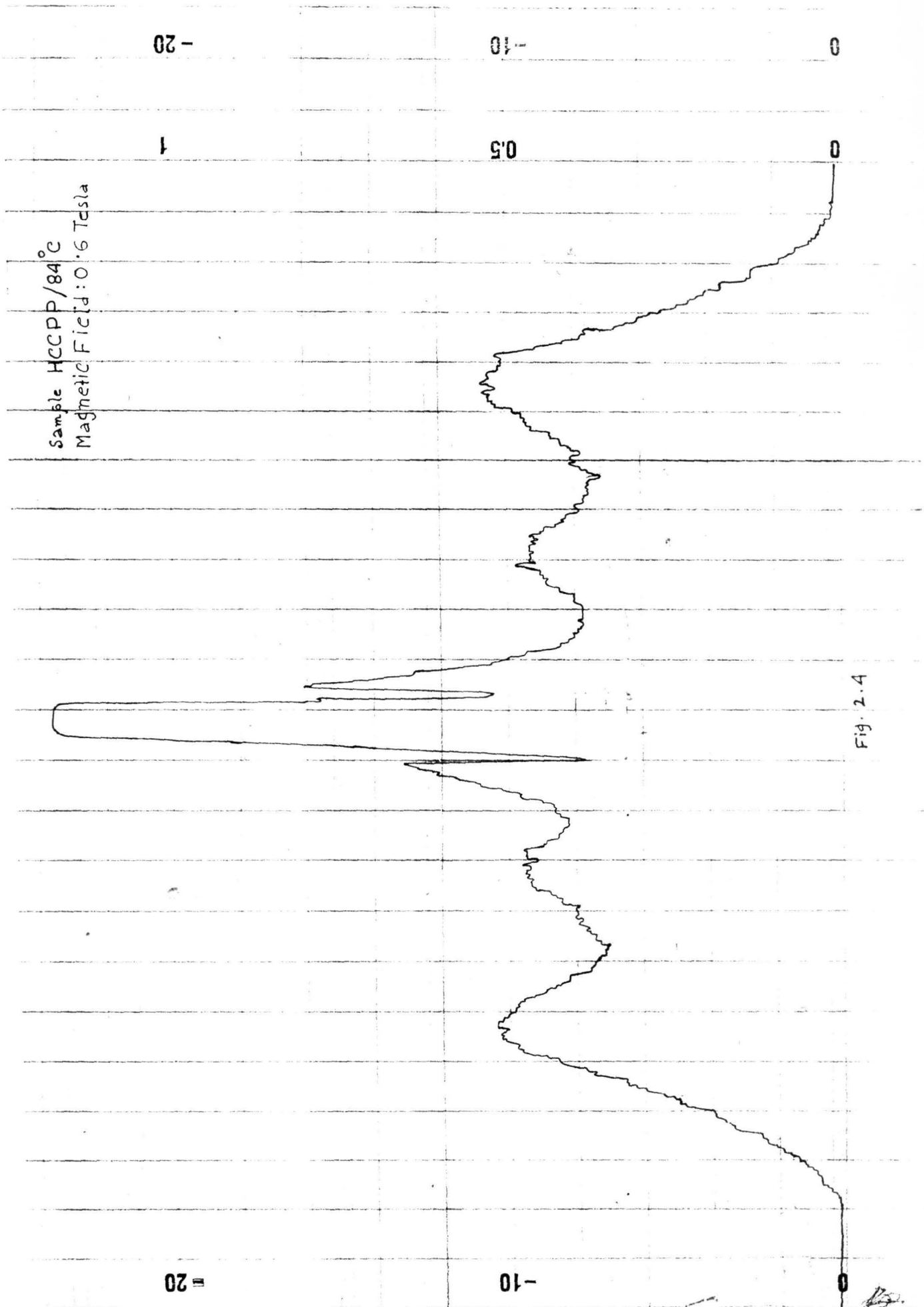
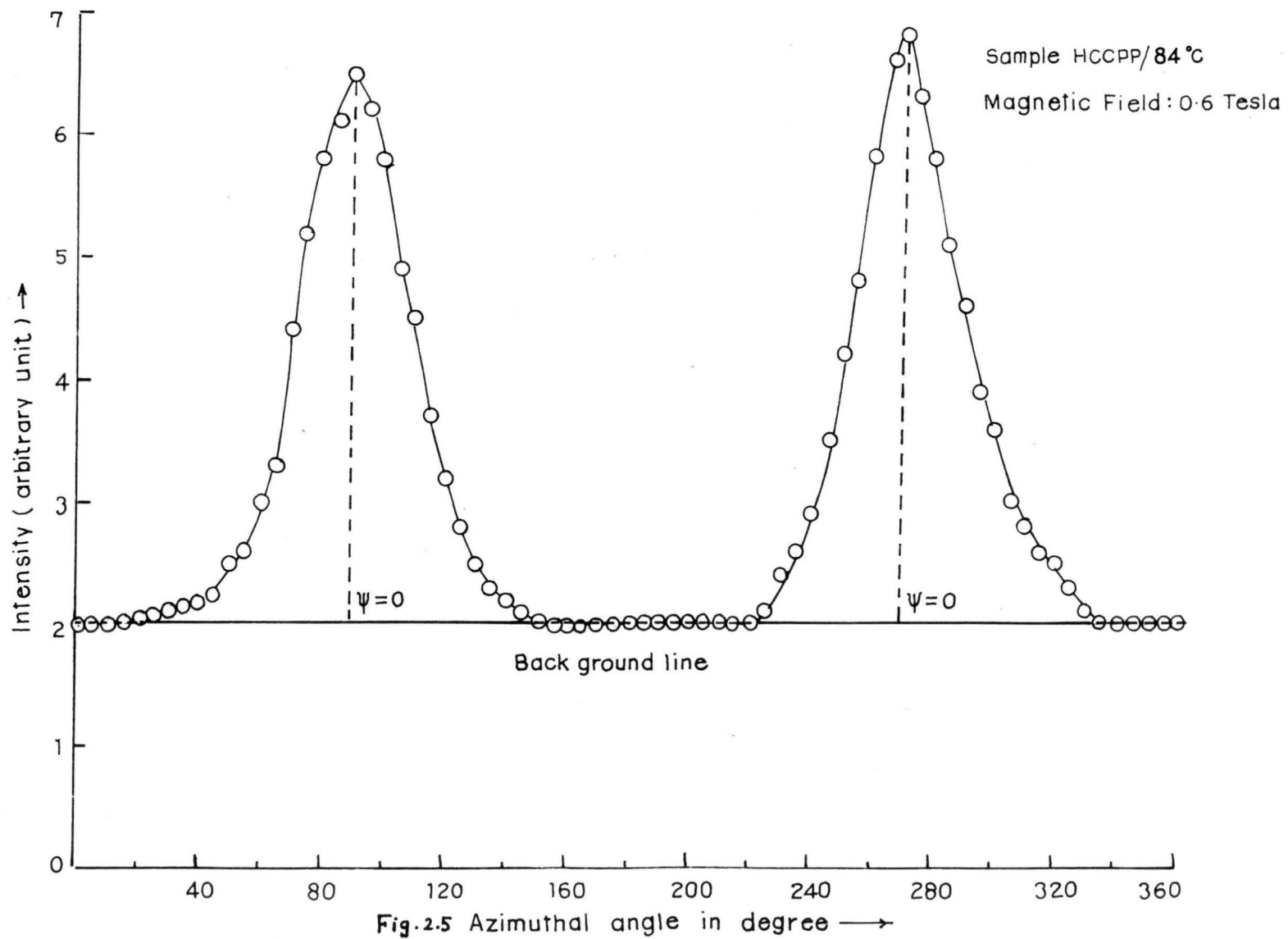


Fig. 2.4



intensity values. The peak intensity position corresponding to $\psi = 0$ was determined (Figure 2.5). However, in some cases some unwanted spots for even a slight non-uniformity in film coating created some problems. In such cases a smooth curve around $\psi = 0$ was drawn very carefully. Mean $I(\psi)$ values of the four quadrants were used to obtain $f(\beta)$, $\langle P_2 \rangle$ and $\langle P_4 \rangle$ values. A computer program has been developed for these calculations.

References

1. H.E.J. Neugebauer, *Canad. J. Phys.*, 32, 1 (1954).
2. M.F. Vuks, *Optics and Spectroscopy*, 20, 361 (1966).
3. P.G. de Gennes, *Mol. Cryst. Liq. Cryst.*, 12, 193 (1971).
4. I. Haller, H.A. Huggins, H.R. Lillenthal and T.R. McGuire, *J. phys. Chem.*, 77, 950 (1973).
5. A.K. Zeminder, S. Paul and R. Paul, *Mol. Cryst. Liq. Cryst.*, 61, 191 (1980).
6. J.S.V.D. Lingen, *Ber. Dt. Chem. Ges.*, 15, 913 (1913).
7. G. Friedel, *Annals. Phys.*, 18, 273 (1922).
8. B.K. Vainshtein, *Diffraction of X-rays by Chain Molecules*, Elsevier Publishing Co., (1966).
9. A.J. Leadbetter, *The Mol. Phys. of Liquid Crystals*, Eds. G.R. Luckhurst and G.W. Gray, Academic Press, Ch. 13, (1979).
10. J.H. Wendorff and E.P. Price, *Mol. Cryst. Liq. Cryst.*, 24, 129 (1973).
11. I.G. Chistyakov, R.I. Schabischev, R.I. Jarenov and L.A. Gusakova, *Mol. Cryst. Liq. Cryst.*, 7, 279 (1969).
12. A. de Vries, *Mol. Cryst. Liq. Cryst.*, 10, 31 and 219 (1970).
13. A. de Vries, *Mol. Cryst. Liq. Cryst.*, 11, 361 (1970); 20, 119 (1973).
14. C. Zannoni, *The Mol. Phys. of Liquid Crystals*, Eds. G. R. Luckhurst and G.W. Gray, Academic Press, Chap. 3, (1979).
15. A.J. Leadbetter and E.K. Norris, *Mol. Phys.*, 38, 669 (1979).
16. P.G. de Gennes, *The Phys. of Liquid Crystals*, Clarendon press, Oxford, Chap. 2, (1974).
17. B. Jha, S. Paul, R. Paul and P. Mandal, *Phase Trans.*, 15, 39 (1989).
18. H.P. Klug and L.E. Alexander, *X-ray diffraction procedures*, John Wiley and Sons, NY, page 114 and 473 (1974).